E6-2002-11

J. Adam[1], J. Dobeš[2], M. Honusek[2], V. G. Kalinnikov,
J. Mrázek[2], V. S. Pronskikh[3], P. Čaloun[1], N. A. Lebedev,
V. I. Stegailov, V. M. Tsoupko-Sitnikov

PROPERTIES OF ^{152}Gd COLLECTIVE STATES
(Comparison of Experimental and Theoretical Results)

Submitted to «European Physical Journal A»

[1]On leave from Nuclear Physics Institute of ASCR, Řež, Czech Republic
[2]Nuclear Physics Institute of ASCR, Řež, Czech Republic
[3]On leave from St. Petersburg State Institute of Technology, Russia

1 Introduction

Nucleus $^{152}_{64}Gd_{88}$ has six neutrons more than the nearest doubly magic nucleus $^{146}_{64}Gd_{82}$, and properties of its excited states should be described with allowance for the pairing force, which spherifies the nucleus, the quadrupole force, which deformes it. Calculations of the deforming energy surface (DES) of ^{152}Gd using the pairing plus quadrupole model (PPQ) by Kumar and Gupta [1] were able to show what shape the nucleus had. For an axially symmetrical nucleus they found that its potential energy had a minimum at β=0.19 for the "prolate" shape, and β=-0.04 for a slightly "oblate" one. This fact suggests that the ^{152}Gd nucleus is quite soft with respect to vibrations, and possibly demonstrates shape coexistence.

First determination of the ^{152}Gd low-energy levels was made by Zolnowski et al. [2]. They compared energies, spins, and pairities of levels in the nucleus, as well as reduced probabilities of their deexciting transitions with those in the neighbouring deformed ^{154}Gd, for which a detailed classification had been made by Meyer [6]. Besides the rotational bands built on the ground, β-, and γ-vibrational states, he also identified such rotational bands on the octupole-vibrational and two-phonon (2β,$\beta\gamma$) states. The authors of [2] introduced this kind of "quasirotational" states in ^{152}Gd. Energies of the levels with negative pairities in isotones with N=88 were studied [3] in comparison with the calculations taking into account quadrupole-octupole coupling (QOC) of collective motion [4, 5]. Good agreement between experimental and calculated values was observed for these levels. The reduced probabilities of the $E2$ transitions and the energies of the low-lying levels with positive parities were calculated in [3] in the framework of a microscopic model using the boson-expansion technique and compared with the experimental ones. The agreement was rather good, but the calculations [1] with the PPQ model gave much better results for $B(E2)$, despite the fact that the residual nucleon-nucleon interaction in both models was described similarly.

2 Phenomenological approaches, Q-phonon model, phase transitions

Energies of rotational and quasirotational bands can be described by a number of phenomenological formulae. The general form of the Bohr-Mottelson [7] equation is given by :

$$E_I = E_0 + \sum_{n=1} A_n [I(I+1)]^n + (-1)^{I+K} \frac{(I+K)!}{(I-K)!} \sum_{m=0} A_m [I(I+1)]^m \,. \quad (1)$$

An additional term reflecting the Coriolis interaction :

$$A_{1/2} \sqrt{I(I+1)} \,, \quad (2)$$

was added to (1) by [8]. In the transitional region, energies of quasirotational bands can also be calculated with formulae of Ejiri [9] :

$$E_I = aI + kI(I+1) \quad (3)$$

or Varshni [10] :

$$E_I = aI + kI(I+1) + qI^2(I+1) \,. \quad (4)$$

In (4), the first term stands for the vibrational motion of the nucleus, the second for the rotational one, while the third reflects the interaction between the former and the latter.

Rotational and quasirotational spectra were described in the framework of the model of a variable momentum of inertia (VMI) [11, 12, 13, 14] based on the forced rotation model [15]. The versions of the VMI differ from one another by methods used for calculation of the potential energy of the nucleus. Possible non-axiality of the nuclear shape was considered in [16, 17]. An approximate analytical solution for hamiltonian eigenvalues of the asymmetric rotor was given [17] :

$$E_{rot} = A[I(I+1) + \alpha I] \,, \qquad \alpha \equiv \left[\left(\frac{A_2}{A_1} - 1 \right) \left(\frac{A_3}{A_1} - 1 \right) \right]^{1/2} \,, \quad (5)$$

where α is the parameter of asymmetry, and A_1, A_2, A_3 are the symmetry axes of the rotor.

Potential energy of the nucleus is defined as in the VMI model [12] :

$$E_{pot} = \left(\frac{C}{2\hbar^4}\right)(\Im - \Im_0)^2 \,, \tag{6}$$

where C is the rigidity parameter of nucleus, the magnitude of which depends on n- and p-pairing correlations as well as on the quadrupole and hexadecapole nuclear deformation parameters. The total energy extremum condition $E = E_{rot} + E_{pot}$ leads to the following approximate analytical equations

$$E_I = \frac{\hbar^2}{2\Im_0}(b_1 I + b_2 I^2 + b_3 I^3)\,, \tag{7}$$

$$\Im_I = \Im_0(1 + B_1 I + B_2 I^2 + B_3 I^3)\,, \tag{8}$$

where $\Im_I$ is the variable momentum of inertia and $\Im_0$ is the momentum of inertia in the ground state.

Having determined the parameters b_1, b_2, and b_3 from the experimental values of E_I and using the equations

$$\begin{aligned} b_1 &\approx 1 + \alpha - 16\sigma\,, \\ b_2 &\approx 1 - (0.5\alpha^2 + 4\alpha + 3.5)\sigma\,, \\ b_3 &\approx -(\alpha + 5)\sigma\,, \end{aligned} \tag{9}$$

where $\sigma \equiv \frac{\hbar^6}{2c\Im_0^3}$ is the non-rigidity parameter of nucleus, one can first find α and σ, and then determine B_1, B_2, and B_3 using the formulae

$$\begin{aligned} B_1 &\approx (\alpha + 1)\sigma\,, \\ B_2 &\approx \sigma\,, \\ B_3 &\approx -4(\alpha + 5)\sigma^2\,. \end{aligned} \tag{10}$$

More exact equations for b_i and B_i, also containing the terms proportional to σ^2 and σ^3, were derived in [17]. Using the values ε_2, ε_4 and

ε_6 (see Table 1) and the following system fo equations

$$\begin{aligned}
\frac{\hbar^2}{2\Im_0} b_1 &= \frac{\varepsilon_2}{2} - \frac{\varepsilon_4}{4} + \frac{\varepsilon_6}{6}\,, \\
\frac{\hbar^2}{2\Im_0} b_2 &= \frac{\varepsilon_4}{8} - \frac{\varepsilon_6}{8}\,, \\
\frac{\hbar^2}{2\Im_0} b_3 &= \frac{\varepsilon_6}{48}\,,
\end{aligned}$$

as well as the ratios $B \equiv b_1/b_3$ and $b \equiv b_2/b_3$, one can obtain from the system (9) the cubic equation for the parameter α

$$\alpha^3 + (9 - 2b)\alpha^2 + (15 + 2B - 12b)\alpha + 10(B - b) - 25 = 0\,,$$

which has only one positive root α=12.723. Thus, from the equation :

$$\sigma = \frac{\alpha + 1}{16 - B(\alpha + 5)}$$

we have σ=0.00101.

Low-lying collective states of a nucleus can also be described in the framework of the Q-phonon model [18], in which wave-functions of excited states are created by applying the quadrupole operator to the wave-function of the ground state. In this model, level energies in "quasirotational" bands are written as

$$E_I = \frac{IE(2_1^+)}{2} + \varepsilon_4 \frac{I(I-2)}{8} + \varepsilon_6 \frac{I(I-2)(I-4)}{48}\,. \qquad (11)$$

With the Q-phonon approach, having measured experimental data on the reduced probabilities of $E2$ transitions $2_g^+ \to 0_g^+$, $4_g^+ \to 2_g^+$, $2_\gamma^+ \to 0_g^+$, $2_\gamma^+ \to 2_g^+$, one can easily calculate several shape invariants and thus gain important information on the structure of a given nucleus.

Lifetimes of the 2_g^+ and 4_g^+ states in ^{152}Gd are known, and it is possible to find on their basis the following quantities :

$$B(E2, 2_g^+ \to 0_g^+) = 0.349(18)\, e^2b^2 \text{ and } B(E2, 4_g^+ \to 2_g^+) = 0.64(4)\, e^2b^2\,.$$

As the lifetime of the 2^+_γ state is not known in this nucleus, the absolute probabilities of the E2 transitions $2^+_\gamma \to 0^+_g$ $2^+_\gamma \to 2^+_g$ can be evaluated [21] by the formula

$$B(E2, 2^+_\gamma \to 0^+_g) \approx \frac{B(E2, 3^+_\gamma \to 2^+_g)}{B(E2, 3^+_\gamma \to 2^+_\gamma)} B(E2, 2^+_g \to 0^+_g) =$$

$$= \left(\frac{E_\gamma(3^+_\gamma \to 2^+_\gamma)}{E_\gamma(3^+_\gamma \to 2^+_g)}\right)^5 \times \frac{I_\gamma(3^+_\gamma \to 2^+_g)\left(\frac{\delta^2}{1+\delta^2}\right)}{I_\gamma(3^+_\gamma \to 2^+_\gamma)\left(\frac{\delta'^2}{1+\delta'^2}\right)} B(E2, 2^+_g \to 0^+_g). \quad (12)$$

Afterwards, $B(E2, 2^+_\gamma \to 2^+_g)$ can be calculated with the equation

$$B(E2, 2^+_\gamma \to 2^+_g) = \left(\frac{E_\gamma(2^+_\gamma \to 0^+_g)}{E_\gamma(2^+_\gamma \to 2^+_g)}\right)^5 \times$$

$$\times \frac{I_\gamma(2^+_\gamma \to 2^+_g)}{I_\gamma(2^+_\gamma \to 0^+_g)} \left(\frac{\delta^2}{1+\delta^2}\right) B(E2, 2^+_\gamma \to 0^+_g). \quad (13)$$

Substituting measured earlier experimental energies E_γ and intensities I_γ of the transitions deexciting ^{152}Gd states [22] and the mixture parameters of [24] in (13) we have

$$B(E2, 2^+_\gamma \to 0^+_g) = 8.1(27) \times 10^{-4}\, e^2b^2 \quad \text{and}$$

$$B(E2, 2^+_\gamma \to 2^+_g) = 5.2(24) \times 10^{-4}\, e^2b^2 .$$

Following the receipt of [18], the reduced probability ratios G, R_1 and W, as well as the relative $q(2^+_g)$ and absolute $|Q(2^+_g)|$ values of the quadrupole momenta of the first excited 2^+_g state were found

$$\begin{aligned}
G &= \frac{7}{10}\frac{B(E2, 4^+_g \to 2^+_g)}{B(E2, 2^+_g \to 0^+_g)} = 1.28(10), \\
R_1 &= \frac{B(E2, 2^+_\gamma \to 0^+_g)}{B(E2, 2^+_g \to 0^+_g)} = 2.3(8) \times 10^{-3}, \\
W &= \frac{B(E2, 2^+_\gamma \to 2^+_g)}{B(E2, 4^+_g \to 2^+_g)} = 8(4) \times 10^{-3}, \\
q(2^+_g) &= \frac{8}{7}\sqrt{\pi G(1 + R_1 - W)} = 2.28(13), \\
|Q(2^+_g)| &= q(2^+_g)\sqrt{B(E2, 2^+_g \to 0^+_g)} = 1.35(9).
\end{aligned}$$

Nuclear shape invariants are introduced in the Q-phonon model as average scalars constructed of various numbers of quadrupole operators. Their values do not change under rotation of the coordinate system. In the geometric approach, the invariants are associated with the nuclear shape parameters β and γ. Dependence of the shape invariants K_2 – K_6 on the reduced probabilities of $E2$ transitions was determined by [25, 26]

$$K_2 \equiv e^2_{\rm eff} < 0^+_g|(QQ)_0|0^+_g >< 0^+_g|\beta^2|0^+_g > \approx$$
$$\approx B(E2, 0^+_g \to 2^+_g) + B(E2, 0^+_g \to 2^+_\gamma) \equiv K_2^{\rm appr} = 1.75(16)\, e^2b^2\,,$$

$$K_3 \equiv \frac{|< 0^+_g|(QQQ)_0|0^+_g >|}{< 0^+_g|(QQ)_0|0^+_g >^{3/2}}\sqrt{5\sqrt{5}} = \sqrt{\frac{2}{35}}\frac{< 0^+_g|\beta^3\cos 3\gamma|0^+_g >}{< 0^+_g|\beta^2|0^+_g >^{3/2}} \approx$$
$$\approx \sqrt{\frac{2G}{35}}\left[\left(\frac{1-R_1}{1+R_1}\right)\sqrt{1-\frac{W}{1+R_1}} - \frac{2}{1+R_1}\sqrt{\frac{R_1W}{1+R_1}}\right] \equiv$$
$$\equiv K_3^{\rm appr} = 0.266(15)\,,$$

$$K_4 \equiv \frac{|< 0^+_g|(QQ)^2_0|0^+_g >|}{< 0^+_g|(QQ)_0|0^+_g >^2} = \frac{|< 0^+_g|\beta^4|0^+_g >|}{< 0^+_g|\beta^2|0^+_g >^2} \approx$$
$$\approx \frac{7}{10}\frac{B(E2, 4^+_g \to 2^+_g)}{B(E2, 2^+_g \to 0^+_g)} = G \equiv K_4^{\rm appr} = 1.28(10)\,.$$

If the effective charge is known, the average deformation parameter β^2 is governed by $K_2^{\rm appr}$ and its fluctuation by $K_4^{\rm appr} - 1$. Similarly, the effective value of γ is found as $\gamma_{\rm eff} = \frac{1}{3}\arccos\left(\sqrt{\frac{35}{2}}K_3^{\rm appr}\right)$, but since only the absolute value of $K_3^{\rm appr}$ was found by us, it is impossible to discriminate between $\gamma_{\rm eff}$ and $\frac{\pi}{3} - \gamma_{\rm eff}$. On the basis of $\sqrt{\frac{35}{2}}K_3^{\rm appr} = 1.11(6)$ calculated for ^{152}Gd, one can conclude that $\gamma^{\rm eff} \approx 0°$ or $60°$.

In this work, for comparison of experimental and theoretical level energies of the ^{152}Gd yrast-band, the following dependencies of level

energies on level spins were used :

$$E_{cal} = AI(I+1) \quad (14)$$

$$E_{cal} = AI(I+1) + BI^2(I+1)^2 \quad (15)$$

$$E_{cal} = CI(I+1) + D\sqrt{I(I+1)} \quad (16)$$

$$E_{cal} = FI + G\sqrt{I} \quad (17)$$

$$E_{cal} = \frac{\varepsilon_2 I}{2} + \frac{\varepsilon_4 I(I-2)}{8} \quad (18)$$

$$E_{cal} = \frac{\varepsilon_2 I}{2} + \frac{\varepsilon_4 I(I-2)}{8} + \frac{\varepsilon_6 I(I-2)(I-4)}{48} \quad (19)$$

$$E_{cal} = a_1 n_d + a_2 n_d(n_d+4) + a_3 v(v+3) + a_4 I(I+1)\,. \quad (20)$$

It is noteworthy that equation (18) is equivalent to the Ejiri formula (3), while (19) can easily be transformed to yield either the Varshni formula (4), or (7), or (11). The results of the fits, the fitted parameters and the averaged residuals of the level energies $< |E_{exp} - E_{calc}| >$ are shown in Table 1. Such analysis was also performed with allowance for the level $I^\pi = 16^+$, whose experimental determination is unreliable. Including it into the yrast-band worsened the average residual of (19) from 2.21 keV to 4.05 keV, almost by two-fold. It is evident from the table that the yrast-band energies of ^{152}Gd are best described by (19).

The energy ratio of the 4_g^+ and 2_g^+ levels in the ^{152}Gd nucleus indicates that it belongs to the transitional region. In figures 1(2) the values of $R^i_{4/2} = E(4_i^+)/E(2_i^+)$ for even Gd isotopes (even N=88 isotones) are shown. The index i=1 denotes the ground state band, i=2(3) stand for bands built on the second (third) 0^+ state. For ^{152}Gd $R^1_{4/2}$=2.1, and this fact suggests the probable position of the nucleus at the critical point of either the first-order phase transition from the vibrator to the γ-unstable (U(5)–SO(6)) shape, or the second-order transition from the vibrator to the deformed (U(5)–SU(3)) shape. A theory for calculation of properties of nuclei close to the critical point of the former (E(5) symmetry) and the latter (X(5) symmetry) was recently proposed by F.Iachello [19, 20]. He points out that there is a new class of

I^π	E(exp)	σ(E)	E(cal)[keV]					
	[keV]	[keV]	(14)	(15)	(16)	(17)	(18)	(19)
2	344.3	0.5	127.4	178.6	387.1	289.5	360.0	344.3
4	755.4	0.5	424.6	575.5	773.7	759.7	768.7	756.6
6	1227.4	0.5	891.8	1143.2	1217.6	1259.7	1226.2	1226.7
8	1746.8	0.5	1528.7	1806.8	1720.1	1775.1	1732.5	1745.2
10	2300.4	0.8	2335.6	2464.4	2281.6	2300.3	2287.4	2302.4
12	2883.8	1.1	3312.3	2986.9	2902.1	2832.5	2891.2	2888.5
14	3499.2	1.5	4458.8	3217.9	3581.9	3370.0	3543.7	3494.0
$< \lvert E(exp) - E(cal) \rvert >$			360	148	31.1	42.9	15.6	2.21
A			21.2	30.2				
B				-0.071				
C					7.40			
D					139.9			
F						299.0		
G						-218.2		
ε_2							360.0	344.4
ε_4							48.8	67.7
ε_6								-9.67

Table 1: Comparison of the experimental ^{152}Gd level energies to calculated ones up to I^π=14^+

dynamic symmetries describing systems undergoing phase transitions, based not on group theoretical description but on "representation symmetries" associated with zeros of special functions. For the differential equation

$$H\Psi = E\Psi$$

with the Bohr Hamiltonian

$$H = -\frac{\hbar^2}{2B}\left[\frac{1}{\beta^4}\frac{\partial}{\partial\beta}\beta^4\frac{\partial}{\partial\beta} + \frac{1}{\beta^2\sin 3\gamma}\frac{\partial}{\partial\gamma}\sin 3\gamma\frac{\partial}{\partial\gamma} - \right.$$
$$\left. - \frac{1}{4\beta^2}\sum_k \frac{Q_k^2}{\sin^2(\gamma - \frac{2}{3}\pi k)}\right] + V(\beta,\gamma)\,,$$

where the potential is taken to be a square well in the variable β and a harmonic oscillator in γ for the X(5) symmetry, and depends only

on β for the E(5). One can obtain the Bessel equation

$$\varphi'' + \frac{\varphi'}{z} + \left[1 - \frac{\nu^2}{z^2}\right]\varphi = 0\,,$$

where $\varphi(\beta) = \beta^{3/2} f(\beta)$, $z = \beta k$.

In this case the energy eigenvalues are fixed by the symmetry and can be expressed in terms of zeros of the Bessel function J_ν, with no free parameters at all :

$$\nu = \tau + \frac{3}{2} \quad \text{for U(5)–SO(6) transition, or} \tag{21}$$

$$\nu = \left(\frac{L(L+1)}{3} + \frac{9}{4}\right)^{1/2} \quad \text{for U(5)–SU(3)}\,. \tag{22}$$

For instance, the energy of the transition $4_g^+ \to 2_g^+$ given in units of the $2_g^+ \to 0_g^+$ transition is defined as

$$R_{4/2} = \frac{E_{4_{1,2}} - E_{0_{1,0}}}{E_{2_{1,1}} - E_{0_{1,0}}} = \frac{\kappa_{1,2}^2 - \kappa_{1,0}^2}{\kappa_{1,1}^2 - \kappa_{1,0}^2}\,,$$

where $E_{L_{\xi,\tau}}$ stands for the energy of a level with spin L, determined as the ξth zero of the Bessel function J of the νth order (ν is found using (21) or (22)), and $\kappa_{\xi,\tau}$ is the ξth zero of the function J_ν. Comparison of the experimental $R_{I/I-2}$ of ^{152}Gd with their theoretical values calculated in [19] and [20] is given in Table 2. Reduced probability ratios calculated in the papers cited above for some $E2$ transitions and their experimental values for ^{152}Gd are shown in Table 3. The calculations were also made without a free parameter. The results of the comparison for $B(E2)$ show preference to neither E(5) nor X(5) symmetry, although the calculated data for E(5) are a little closer to the experimental ones. On the other hand, the experimental $R_{I/I-1}$ almost coincide with the calculated ones if E(5) symmetry is assumed and significantly differ from them in the case of X(5). Also, the ratio $E(0_2^+)/E(2_1^+)$ calculated for E(5) symmetry is very close to its experimental value for $E(0_3^+)/E(2_1^+)$ (see Table 2).

In this connection a question arises as to the nature of the quasirotational band built on the first excited 0^+ state of ^{152}Gd and its possible

	$R_{4/2}$	$R_{6/2}$	$R_{8/2}$	$R_{10/2}$	$R_{12/2}$	$R_{14/2}$	$\frac{E(0_2^+)}{E(2_1^+)}$	$\frac{E(0_3^+)}{E(2_1^+)}$	$\frac{E(0_4^+)}{E(2_1^+)}$
^{152}Gd(exp)	2.194	3.565	5.074	6.682	8.376	10.164	1.787	3.043	
E(5)	2.199	3.590	5.169	6.934	8.881	11.009	3.03		7.5
X(5)	2.904	5.430	8.483	12.027	16.041	20.514	5.67	14.1	

Table 2: Experimental and theoretical level energy ratios for ^{152}Gd

	$\frac{B(E2,4_g^+\to 2_g^+)}{B(E2,2_g^+\to 0_g^+)}$	$\frac{B(E2,6_g^+\to 4_g^+)}{B(E2,2_g^+\to 0_g^+)}$	$\frac{B(E2,0^+\to 2_g^+)}{B(E2,2_g^+\to 0_g^+)}$	$\frac{B(E2,2_\beta^+\to 0_3^+)}{B(E2,2_g^+\to 0_g^+)}$
^{152}Gd(exp)	1.83(15)	2.72(56)	2.46(53)	0.49
E(5)	1.68	2.21	0.86	0.75
X(5)	1.58	1.98	0.63	0.79

Table 3: Experimental and theoretical reduced probability ratios for ^{152}Gd

"intruder" origin. This fact spurred us to perform various calculations in the framework of the IBA-2 model under different assumptions of the nature of this state. That $(R_{I/I-2})_{exp}$ is close to its theoretical values for E(5) symmetry seems to be rather unpredictable and proves complexity of the transition from the spherical to the deformed nuclear shape.

3 Interacting Boson Model (IBA)

Energies of the quasirotational bands and transition properties ($B(E2)$, $\rho(E0)$, $X(E0/E2)$) were calculated in [27] by the projection model and IBA-1. The comparison showed that the both models reproduced the level energies quite well, reduced probabilities of the $E2$ transitions satisfactorily, and those for $E0$ transitions badly. The IBA-1 model with seven parameters was used [28] for description of electromagnetic properties of five N=88 nuclei with the same set of parameters employed for all of them. Several nuclei were analyzed [29] in the U(5) limit of IBA-1. The excitation energy ratios of ^{152}Gd $R_{4/2}^{calc}$=2.03 ($R_{4/2}^{exp}$=2.19), and the reduced probability ratios were found to be $\frac{B(E2,4^+\to 2^+)}{B(E2,2^+\to 0^+)}$ = 1.83 (calculated) and 1.9 (experimental). In spite of such good agreement for the 2_g^+ and 4_g^+ levels, the authors of [29]

conclude that the ^{152}Gd nucleus cannot be considered as only vibrational as the predicted excitation energy of the 0_3^+ level was 1425 keV, while the observed one was 1047.77 keV. In this case this level could be the head level of the "intruder" band, but no more 0^+ states with the energy higher than 1048 keV were observed.

Calculations of $B(E2)$, $B(M1)$ and δ for ^{152}Gd by the least squares method applied to some of parameters within the nine-parameter IBA-2 model were performed [24] on the basis of the experimental transition energies. The following Hamiltonian was used by them :

$$H = \varepsilon(\hat{n}_{d\nu} + \hat{n}_{d\pi}) + \kappa Q_\nu Q_\pi + \bar{\kappa}(Q_\nu Q_\nu + Q_\pi Q_\pi) + V_{\nu\nu} + V_{\pi\pi} + M_{\nu\pi},$$

where

$$\hat{n}_{d\rho} = d_\rho^+ \cdot \tilde{d}_\rho \ .$$

is the operator of the d-boson number for protons (ρ=π) or neutrons (ρ=ν). Here s^+ and $\tilde{s}$ (d^+ and $\tilde{d}$) are operators of s (d) bosons. The quadrupole operator Q_ρ has the form :

$$Q_\rho = (d_\rho^+ \tilde{s}_\rho + s_\rho^+ \tilde{d}_\rho)^{(2)} + \chi_\rho (d_\rho^+ \tilde{d}_\rho)^{(2)} \quad \rho = \pi, \nu \quad .$$

The Majorana operator is

$$M_{\nu\pi} = \frac{1}{2}\xi_2 (s_\nu^+ d_\pi^+ - d_\nu^+ s_\pi^+)^{(2)} (\tilde{s}_\nu \tilde{d}_\pi - \tilde{d}_\nu \tilde{s}_\pi)^{(2)} - \sum_{k=1,3} \xi_k (d_\nu^+ d_\pi^+)^{(k)} (\tilde{d}_\nu \tilde{d}_\pi)^{(k)} , \tag{23}$$

and the interaction between $n-n$ and $p-p$ quasi-bosons is

$$V_{\rho\rho} = \frac{1}{2} \sum_{L=0,2,4} c_{L\rho} (d_\rho^+ \tilde{d}_\rho)_L (d_\rho^+ \tilde{d}_\rho)_L \ . \tag{24}$$

Excitation of identical nucleon pairs in excess of the closed shells can also be taken into account in the IBA [30]. For instance, such excitation of a pair of protons increases the proton boson number by two.

The Hamiltonian of the model also contains the additional term

$$H_{mix} = \alpha (s_\rho^+ s_\rho^+ + s_\rho s_\rho)^{(0)} + \beta \ (d_\rho^+ d_\rho^+ + \tilde{d}_\rho \tilde{d}_\rho)^{(0)} \ . \tag{25}$$

We examined three hypotheses on the structure of ^{152}Gd excited states in this work. Besides the structure proposed in [31], where the β-band is built on the 615.37 keV (0^+) level (version I), we considered the scheme with a β-band built on the 1047.77 keV (0^+) level and the 615.37 keV level as an "intruder" (version II), and also the scheme with the 1047.77 keV band as the "intruder" one (version III). The level energies were calculated with the help of the QHINT [32] package, adopted and modified at NPI ASCR, Řež. Calculations by an analytical equation with four free paramerets corresponding to the vibrational limit O(6) of IBA-2 (20) were also carried out. The results of the calculation and the parameters determined from experiment are given in Table 6 as version IV. The smallest discrepancies between the experimental and theoretical energies were for version III. The energies and reduced probabilities for version II were determined by direct fitting of the IBA parameters on the basis of the experimental β-band energies followed by calculations with QHINT using these parameters. The parameters used are given in Tables 4 and 5.

version	ε	κ	χ_π	χ_ν	C_0^π	C_2^π	ξ_1	ξ_2	ξ_3
ver I.	0.73	-0.07	-2.0	-0.4	-0.2	-0.1	0.25	0.25	0.25
ver II.	0.741	-0.117	-0.602	-0.536	0	0	0.3	0.05	0.3
ver III.	0.6896	-0.0590	-1.9460	-0.40	-0.2	-0.1	0.25	0.25	0.25

Table 4: The IBA-2 parameters for ^{152}Gd

version	$e2_\pi$	$e2_\nu$	$e0_\pi$	$e0_\nu$
ver I.	0.12703	0.05828	-0.00132	-0.00026
ver II.	0.12129	0.11322	-0.00224	0.00195
ver III.	0.17347	-0.16012	-0.00738	0.02374

Table 5: The IBA-2 charges for ^{152}Gd

Experimental level energies, γ-ray energies and intensities and total intensities of transitions in ^{152}Gd were taken from our papers [22, 23]. Reduced probability ratios were calculated by equation (13) with the mixture parameters δ taken from [24]. Measured level lifetimes $T_{1/2}^{lev}$ for calculation of absolute experimental $B(E2)$ $[e^2b^2]$ [s] were extracted

from [9] :

$$B(E2, I_i \to I_f) = 81.61 \times \frac{\ln 2}{T^{lev}_{1/2}} \frac{I_\gamma(I_i \to I_f)}{E^5_\gamma \sum_{k=1}^{i-1} I^{tot}_{ik}} \times \frac{\delta^2}{1+\delta^2},$$

where E_γ is in keV. Experimental values of absolute $B(E2)$ are given in Table 7 together with the data calculated in this work and published earlier. Theoretical and experimental reduced probability ratios are shown in Tables 8 – 15. Monopole moments $\rho(E0)$ and Rasmussen parameters $X(E0/E2)$ are given in Tables 16 and 17. In order to estimate the difference between the calculated and experimental results, we determined the averaged residuals as

$$\bar{x} = \sum_{i=1}^{n} \frac{1}{n} \frac{|x_{exp}(i) - x_{theo}(i)|}{x_{exp}(i)}, \tag{26}$$

where $x_{exp}(i)$ ($x_{theo}(i)$) stands for the ith experimental (calculated) value represented in Tables 8 to 16.

Let us first consider versions I, II, and III of our calculations with the IBA-2 model. The averaged residuals for 18 values of $B(E2)$, $\rho(E0)$, and $X(E0/E2)$ do not exceed 60% for versions I and II, whereas for version III they are approximately two times as large. The values of $\bar{x}$ for the $B(E2)$ ratios of transitions deexciting the quasirotational bands were found to be significantly larger in versions I and II (3500% and 2600%), and the largest (9400%) in version III. In the latter case large residuals were obtained for transitions from all bands except the β band. The analysis shows that preference should be given to versions I and II rather than to version III.

Calculations made in earlier works were not complete, except for [1], where rather good agreement was observed between theory and experiment for reduced probabilities, but very bad for level energies.

4 Conclusion

As a result of the comparison performed in this work, we found that the best description of experimental energies of the yrast band levels

^{152}Gd can be obtained in the framework of the Q-phonon model and the model of the variable momentum of inertia with dynamic asymmetry. Satisfactory agreement with experiment was not obtained in calculations with the IBA-2 model. Level energy ratios within the yrast band $R_{I/2}$ were found to be rather close to the calculations for the first-order (E(5)) phase transitions at the critical point [19, 20, 33, 34], carried out without free parameters.

Absolute reduced probabilities and their ratios for the transitions within and outside quasirotational bands were best described with the PPQ [1] model. Within the model IBA-2, the agreement observed for level schemes I and II was better than that for level scheme III case of reduced probabilities and worse in the case of energies. We also tried some other sets of parameters for version I, but they gave improvement only for energies, while description of reduced probabilities was not so good.

J.D. acknowledges support from GACR Grant No. 202/99/0149. This work was also partially supported by the Russian Foundation for Basic Research.

Table 6: Ver I, Ver II, Ver III – IBA-2 calculations, Ver IV – O(6) limit (equation 20).

	E(exp)	σ(E(exp))	Ver I	Ver II	Ver III	Ver IV
0_2^+	615.4	0.5	633.4	539.2	582.8	683.5
0_3^+	1047.8	0.5	1411.3	1070.9	1000.4	
2_1^+	344.3	0.5	314.7	279.6	334.2	405.0
2_2^+	930.6	0.5	934.0	887.7	870.6	807.3
2_3^+	1109.2	0.5	1195.3	1039.4	1105.3	1060.5
2_4^+	1318.4	0.5	1752.4	1546.6	1408.5	
3_1^+	1434.0	0.5	1489.0	1543.0	1407.4	1229.3
4_1^+	755.4	0.5	723.6	723.6	740.3	833.5
4_2^+	1282.3	0.5	1420.1	1379.4	1337.6	1244.2
4_3^+	1550.2	0.5	1751.1	1624.6	1631.3	1663.5
5_1^+	1861.6	0.5	2029.4	2207.0	1924.9	
6_1^+	1227.4	0.5	1229.4	1303.2	1227.9	1285.4
6_2^+	1668.1	0.5	1979.6	1995.3	1871.2	1704.7
$< \lvert E(exp) - E(cal) \rvert >$			142.0	120.0	53.0	75.7

Table 7: Comparison of experimental and calculated absolute B(E2) values (in e^2b^2) for ^{152}Gd

	$2_g^+ \to 0_g^+$	$4_g^+ \to 2_g^+$	$6_g^+ \to 4_g^+$	$2_\beta^+ \to 0_\beta^+$	$2_\beta^+ \to 0_g^+$	$2_\beta^+ \to 2_g^+$	$2_\beta^+ \to 4_g^+$	$0_\beta^+ \to 2_g^+$	$2_\gamma^+ \to 0_g^+$
Experiment	0.349(18)	0.64(4)	0.95(19)	0.171(14)	0.00138(11)	0.084(7)	0.096(8)	0.86(18)	
Present IBA-2, v.I	0.2403	0.4643	0.5911	0.2186	0.0015	0.0871	0.1316	0.4844	0.0025
Present IBA-2, v.II	0.3692	0.5639	0.6485	0.2247	0.0007	0.0033	0.0051	0.0068	0.0125
Present IBA-2, v.III	0.1188	0.2873	0.4149	0.1451	0.0011	0.0731	0.1762	0.5030	0.0016
Tagziria [2] IBA-2	0.33	0.64	0.81	0.30	0.002	0.12	0.18	0.67	
Tagziria [2] DDM	0.40	0.65	0.79	0.39	0.002	0.004	0.03		
Kumar [1] PPQ	0.326				0.009	0.70			0.0114
Lipas [9] IBA-1	0.333				0.00128				0.0124
Lipas [9] PMI	0.333				0.0101				0.0213
Lipas [9] PMA	0.333				0.00823				0.0376

Table 8: B(E2) branching ratios for transitions from the β-band of ^{152}Gd

	$E_{lev}(4^+_\beta)$=1282.27 keV			$E_{lev}(6^+_\beta)$=1668.1 keV		
	$\frac{4^+_\beta \to 2^+_g}{4^+_\beta \to 4^+_g}$	$\frac{4^+_\beta \to 6^+_g}{4^+_\beta \to 4^+_g}$	$\frac{4^+_\beta \to 2^+_\beta}{4^+_\beta \to 4^+_g}$	$\frac{6^+_\beta \to 4^+_\beta}{6^+_\beta \to 6^+_g}$		
Experiment	0.0346(15)	< 6000	6.67(22)	16.6*		
Present IBA-2, v.I	0.001	2.178	6.815	14.327		
Present IBA-2, v.II	0.558	2.984	185.229	274.477		
Present IBA-2, v.III	0.083	3.240	4.234	8.581		
Kumar [1] PPQ	0.01	1.26	8.1	13.9		
Lipas [9] IBA-1	0.11		5.96			
Lipas [9] PMI	0.43		35.8			
Lipas [9] PMA	0.69		14.3			
Zolnowski [5], BE6	0.054		2.6	6.4		

Table 9: B(E2) branching ratios for transitions from the γ-band of ^{152}Gd

	$E_{lev}(2^+_\gamma)$=1109.19 keV				$E_{lev}(3^+_\gamma)$=1434.02 keV		
	$\frac{2^+_\gamma \to 0^+_g}{2^+_\gamma \to 2^+_g}$	$\frac{2^+_\gamma \to 4^+_g}{2^+_\gamma \to 2^+_g}$	$\frac{2^+_\gamma \to 0^+_\beta}{2^+_\gamma \to 0^+_g}$	$\frac{2^+_\gamma \to 2^+_\beta}{2^+_\gamma \to 2^+_g}$	$\frac{3^+_\gamma \to 2^+_g}{3^+_\gamma \to 4^+_g}$	$\frac{3^+_\gamma \to 2^+_\beta}{3^+_\gamma \to 2^+_g}$	$\frac{3^+_\gamma \to 2^+_\gamma}{3^+_\gamma \to 2^+_g}$
Experiment	2.5(6)	8.4(19)	3.18(9)	108(25)	0.375(14)	3.41(12)	19.9(10)
Present IBA-2, v.I	0.544	13.027	22.059	76.071	0.314	11.73	66.682
Present IBA-2, v.II	0.066	0.004	0.129	0.024	0.32	0.147	14.901
Present IBA-2, v.III	36.868	1709.847	26.454	5386.942	0.034	122.783	705.040
Tagziria [2] IBA-2							
Tagziria [2] DDM							
Kumar [1] PPQ	0.33	1.0	3.5	8.0	0.9	1.7	17
Lipas [9] IBA-1	0.06	2.46			0.387		
Lipas [9] PMI	0.38	0.003			0.980		
Lipas [9] PMA	0.38	0.005			1.89		
Zolnowski [5], BE6	0.77	4.8	8.2	11.1	0.8	2.8	

Table 10: γ-band (continued)

	$E_{lev}(4^+_\gamma)$=1550.15 keV			$E_{lev}(5^+_\gamma)$=1861.7 keV		
	$\frac{4^+_\gamma \to 4^+_g}{4^+_\gamma \to 2^+_g}$	$\frac{4^+_\gamma \to 2^+_\gamma}{4^+_\gamma \to 2^+_g}$	$\frac{4^+_\gamma \to 3^+_\gamma}{4^+_\gamma \to 2^+_\gamma}$	$\frac{5^+_\gamma \to 6^+_g}{5^+_\gamma \to 4^+_g}$	$\frac{5^+_\gamma \to 4^+_\beta}{5^+_\gamma \to 4^+_g}$	$\frac{5^+_\gamma \to 3^+_\gamma}{5^+_\gamma \to 4^+_g}$
Experiment	12.5(6)	62(4)	8000(?)	5.4(5)*	2.00(20)*	38(3)*
Present IBA-2, v.I	3.632	265.556	0.923	5.725	7.014	136.597
Present IBA-2, v.II	199.628	445.319	0.583	7.078	0.101	29.781
Present IBA-2, v.III	0.117	121.821	1.172	1499.288	1830.954	46381.557
Tagziria [2] IBA-2						
Tagziria [2] DDM						
Kumar [1] PPQ	2.7	36	1.2	1.6	1.2	19
Lipas [9] IBA-1	9.21					
Lipas [9] PMI	47.1					
Lipas [9] PMA	5.96					
Zolnowski [5], BE6	1.4	8.3	0.44	1.15	0.44	4.7

Table 11: B(E2) branching ratios for transitions from the 0^+_3 band of ^{152}Gd

	$E_{lev}(0^+_3)$=1047.77 keV	$E_{lev}(2^+_4)$=1318.35 keV					
	$\frac{0^+_3 \to 2^+_\beta}{0^+_3 \to 2^+_g}$	$\frac{2^+_4 \to 0^+_g}{2^+_4 \to 2^+_g}$	$\frac{2^+_4 \to 4^+_g}{2^+_4 \to 2^+_g}$	$\frac{2^+_4 \to 0^+_\beta}{2^+_4 \to 0^+_g}$	$\frac{2^+_4 \to 0^+_\beta}{2^+_4 \to 2^+_\beta}$	$\frac{2^+_4 \to 2^+_\beta}{2^+_4 \to 2^+_g}$	$\frac{2^+_4 \to 2^+_\gamma}{2^+_4 \to 2^+_g}$
Experiment	257(7)	$0.046^{+0.356}_{-0.01}$	$0.80^{+6.3}_{-0.28}$	74(4)	0.117(7)	630(40)	61^{+480}_{-21}
Present IBA-2, v.I	3972.402	0.79	0.001	4.475	0.026	136.662	2059.475
Present IBA-2, v.II	0.111	28.397	349.139	0.08	0.008	272.218	230.795
Present IBA-2, v.III	783.713	25.518	25.560	5.957	0.545	278.975	4398.477
Kumar [1] PPQ	105	0.01	0.03	315	0.05	43	130
Zolnowski [5], BE6	20.7						

Table 12: 0_3^+-band (continued)

	$E_{lev}(0_3^+)$=1318.35 keV				$E_{lev}(2_4^+)$=1692.42 keV	
	$\frac{2_4^+ \to 2_\beta^+}{2_4^+ \to 2_\gamma^+}$	$\frac{2_4^+ \to 0_3^+}{2_4^+ \to 0_g^+}$	$\frac{2_4^+ \to 0_3^+}{2_4^+ \to 0_\beta^+}$	$\frac{2_4^+ \to 0_3^+}{2_4^+ \to 2_g^+}$	$\frac{4_4^+ \to 4_g^+}{4_4^+ \to 2_g^+}$	
Experiment	0.471(27)	1470(300)	64(13)	214^{+1680}_{74}	1.17(5)	
Present IBA-2, v.I	0.066	5037.104	125.485	3977.366	5.048	
Present IBA-2, v.II	1.179	39.392	490.499	1118.611	0.186	
Present IBA-2, v.III	0.063	435.550	73.112	11114.522	0.651	
Kumar [1] PPQ	0.3			113		

Table 13: B(E2) branching ratios for transitions from the "2γ"-band of ^{152}Gd

	$E_{lev}(2_5^+)$=1605.58 keV						
	$\frac{2_5^+ \to 0_g^+}{2_5^+ \to 2_g^+}$	$\frac{2_5^+ \to 4_g^+}{2_5^+ \to 2_g^+}$	$\frac{2_5^+ \to 0_\beta^+}{2_5^+ \to 0_g^+}$	$\frac{2_5^+ \to 0_\beta^+}{2_5^+ \to 2_\beta^+}$	$\frac{2_5^+ \to 2_\beta^+}{2_5^+ \to 2_g^+}$	$\frac{2_5^+ \to 2_\gamma^+}{2_5^+ \to 2_g^+}$	$\frac{2_5^+ \to 2_\beta^+}{2_5^+ \to 2_\gamma^+}$
Experiment	$\geq$7.4	$\geq$24	36(6)	0.24(6)	$\geq$1110	$\geq$1720	0.65(17)
Present IBA-2, v.I	1.135	2.604	6.332	0.698	10.291	13.536	0.76
Present IBA-2, v.II	0.666	12.261	11.033	0.045	163.387	21.764	7.507
Present IBA-2, v.III	0.514	2.514	5.911	0.488	6.225	91.883	0.068
Kumar [1] PPQ	0.075	2.8	60	0.08	60	89	0.7

Table 14: "2γ"-band (continued)

	$E_{lev}(2_5^+)$=1605.58 keV			$E_{lev}(3_2^+)$=1839.70 keV			
	$\frac{2_5^+ \to 0_g^+}{2_5^+ \to 0_g^+}$	$\frac{2_5^+ \to 0_3^+}{2_5^+ \to 0_\beta^+}$	$\frac{2_5^+ \to 0_3^+}{2_5^+ \to 2_g^+}$	$\frac{3_2^+ \to 2_g^+}{3_2^+ \to 4_g^+}$	$\frac{3_2^+ \to 2_g^+}{3_2^+ \to 2_\beta^+}$	$\frac{3_2^+ \to 2_g^+}{3_2^+ \to 2_\gamma^+}$	$\frac{3_2^+ \to 2_\beta^+}{3_2^+ \to 2_\gamma^+}$
Experiment	64(9)	1.79(18)	$\geq$470	0.47(12)	0.069(4)	0.096(20)	1.39(28)
Present IBA-2, v.I	1841.103	290.739	2089.821	0.057	0.077	0.015	0.195
Present IBA-2, v.II	54.087	4.902	36.032	0.855	0.025	0.128	5.179
Present IBA-2, v.III	2.873	0.486	1.477	11.634	46.437	0.186	0.004
Kumar [1] PPQ	1900	31		0.005	0.0001	0.0001	1.2

Table 15: "2γ"-band (continued)

	$E_{lev}(3_2^+)$=1839.70 keV		
	$\frac{3_2^+ \to 2_4^+}{3_2^+ \to 2_5^+}$	$\frac{3_2^+ \to 2_4^+}{3_2^+ \to 2_\beta^+}$	$\frac{3_2^+ \to 4_\beta^+}{3_2^+ \to 2_\beta^+}$
Experiment		$\leq$1.2	3.6(7)
Present IBA-2, v.I	0.209	1522.577	12.783
Present IBA-2, v.II	0.184	3.726	5.975
Present IBA-2, v.III	0.008	32.228	35.143
Kumar [1] PPQ	12	27	2.4

Table 16: Experimental and theoretical E0 properties, electric monopole moments, ρ(E0), and X(E0/E2) values of ^{152}Gd. All quantities were multiplied by 100.

$I_i^\pi \to I_f^\pi$	ρ(E0) for transition								
	$0_\beta^+ \to 0_g^+$	$2_\beta^+ \to 2_g^+$	$4_\beta^+ \to 4_g^+$	$0_3^+ \to 0_g^+$	$0_3^+ \to 0_\beta^+$	$2_4^+ \to 2_g^+$	$2_4^+ \to 2_\beta^+$	$2_5^+ \to 2_g^+$	$2_5^+ \to 2_\beta^+$
E_γ [keV]	615.6	586.27	526.85	1047.9	432.5	974.05	387.80	1261.32	675.01
Experiment	6.6(14)	4.6(4)							
Present IBA-2, v.I	3.79	3.12	3.66	0.0000	6.47	0.0000	4.06	0.002	0.027
Present IBA-2, v.II	0.05	0.14	0.25	3.84	0.31	7.57	0.6	1.42	0.03
Present IBA-2, v.III	18.36	1.48	2.19	0.01	0.02	1.14	3.44	1.77	0.43
Kumar [1] PPQ	25	24	24	3	31	5.4	26	7.3	5.6
IBA-1 Lipas [9]	7.0	16.4	23.8						
PMI Lipas [9]	22.9	23.2	23.7						

Table 17: (continued)

$I_i^\pi \to I_f^\pi$	X(E0/E2) for transition							
	$2_\beta^+ \to 2_g^+$	$4_\beta^+ \to 4_g^+$	$0_3^+ \to 0_g^+$	$0_3^+ \to 0_\beta^+$	$2_4^+ \to 2_g^+$	$2_4^+ \to 2_\beta^+$	$2_5^+ \to 2_g^+$	$2_5^+ \to 2_\beta^+$
E_γ [keV]	586.27	526.85	1047.9	432.5	974.05	387.80	1261.32	675.01
Experiment	6.8(5)	24.2(19)	6.9(7)	2.25(23)		36(8)		
Present IBA-2, v.I	6.03	12.95	6.92	3.62	0.34	102.45	135.41	181.6
Present IBA-2, v.II	7.19	22.12	3.9	2.8	8462.24	2.45	310.14	0.04
Present IBA-2, v.III	3.42	7.5	6.96	0.03	38471.37	415.06	366.77	14.32
Tagziria [2] IBA-2								
Kumar [1] PPQ	10.6	16.5			22	12	430	4.2
IBA-1 Lipas [9]	6.9	12.2						
PMI Lipas [9]	52.8	86.5						

Table 18: Average parameters, calculated with equation (26)

Model	$B(E2)$		$B(E2)$ branching ratios								$\rho(E0)$		$X\left(\frac{E0}{E2}\right)$	
	γ-band		2γ-band		β-band		0_3^+-band							
	$\bar{x}$	n	$\bar{x}$	n	$\bar{x}$	n	$\bar{x}$	n	$\bar{x}$	n	$\bar{x}$	n	$\bar{x}$	n
IBA-2, v.I	0.34	8	1.74	13	91.99	16	0.54	4	7.68	12	0.38	2	0.61	5
IBA-2, v.II	0.52	8	2.23	13	1.59	16	14.60	4	89.30	12	0.98	2	0.39	5
IBA-2, v.III	0.44	8	212	13	46.35	16	0.80	4	59.70	12	1.23	2	2.54	5
Tagziria [24],IBA-2	0.37	8												
Tagziria [24], DDM	0.52	7												
Kumar [1], PPQ	4.31	3	0.66	13	5.01	15	0.52	4	1.01	9	2.51	2	0.52	3
Lipas [27], IBA-1	0.06	2	0.50	4			1.14	2			2.63	2	0.25	2
Lipas [27], PMI	3.19	2	1.56	4			7.90	2			2.64	2	4.66	2
Lipas [27], PMA	2.51	2	1.60	4			10.02	2						
Zolnowski [3], BE6			0.84	12			0.59	3	0.92	1				

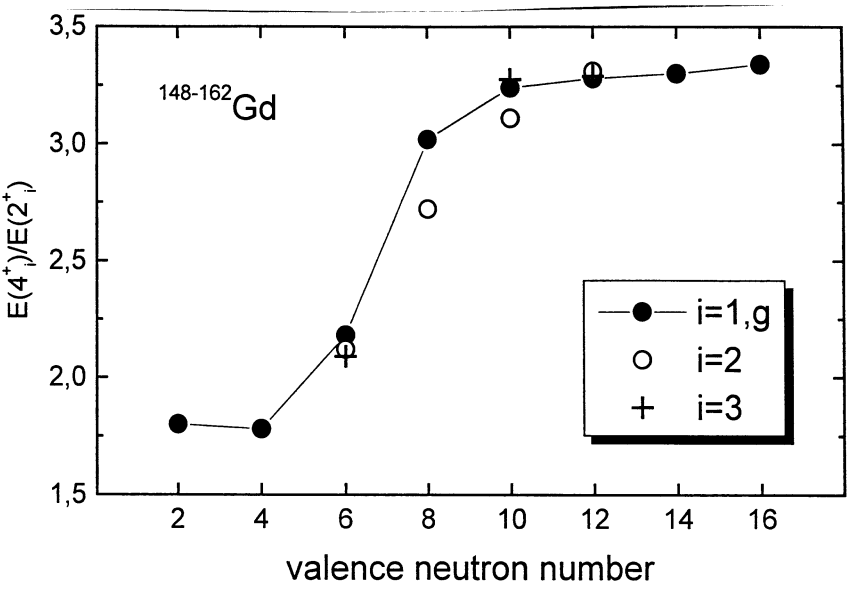

Figure 1. Ratios $R^{i}_{4/2} = E(4_i^+)/E(2_i^+)$ for the even Gd isotopes.

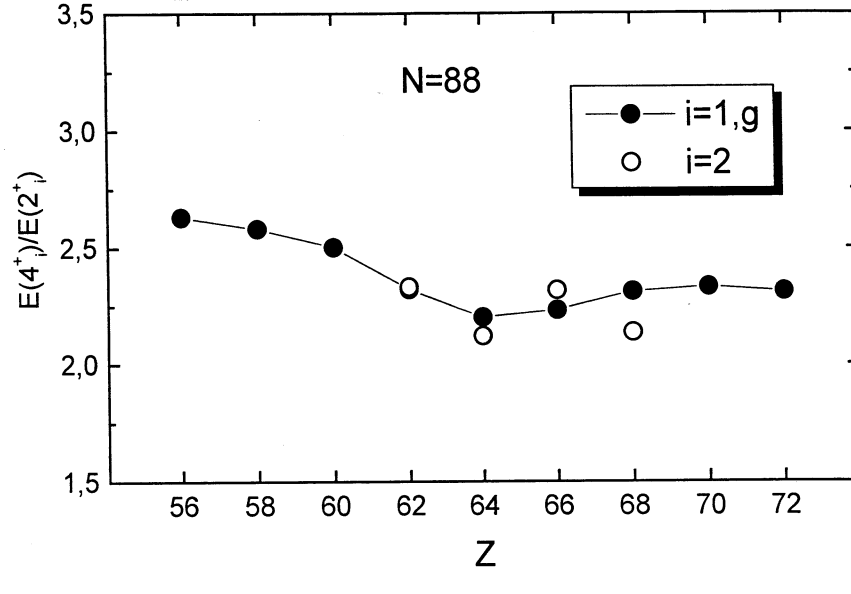

Figure 2. Ratios $R^{i}_{4/2} = E(4_i^+)/E(2_i^+)$ for the even N=88 isotones.

References

[1] K.Kumar, J.B.Gupta, J.Phys. G10(1984)525.

[2] D.R.Zolnowski, E.G.Funk, J.W.Mihelich, Nucl. Phys. A177(1971)513.

[3] D.R.Zolnowski, M.B.Hughes, J.Hunt, T.T.Sugihare, Phys. Rev. C21(1980)2556.

[4] D.R.Zolnowski, T.Kishimoto, Y.Gono, T.T.Sugihare, Phys. Lett. 55B(1975)453.

[5] M.Nomura, Phys. Lett. 55B(1975)357.

[6] R.A.Meyer, Phys. Rev., 170(1968)4.

[7] A.Bohr, B.R.Mottelson, "Nuclear Structure" (W.A.Benjamin, Inc., NY), 1969.

[8] L.K.Peker, S.Pearlstein, J.O.Rasmussen, J.H.Hamilton, Phys. Rev. Lett., 1983.

[9] H.Ejiri, Phys. Soc. Japan, 1968, v.24, p.1181.

[10] Y.Varshni, Progr. Theor. Phys., 1968, v.40.

[11] S.M.Harris, Phys. Rev. Lett., 1964, v.13, p.663; Phys. Rev., 1965, B138, p.509.

[12] M.A.Mariscotti, Phys. Rev., 1969, v.178, p.1864; Phys. Rev. Lett., 1970, v.24, p.1242.

[13] G.Scharff-Goldhaber, C.Dover, A.Goodman, Ann. Rev. Nucl. Sci., 1976, v.26, p.239.

[14] R.M.Diamond, Phys. Lett., 1964, v.11, p.315.

[15] D.R.Inglis, Phys. Rev., 1954, v.96, p.1059.

[16] S.M.Abecasis, E.S.Hernsnoler, Nucl. Phys., 1972, v. A180, p.485.

[17] R.B.Begzhanov, V.M.Bilenkii, E.I.Volmianskii, Izv.AN SSSR (ser.fiz.), 1979, v.43, p.2327.

[18] R.V.Jolos, Jadernaya Fisika, v.64, N3, 2001, p.520.

[19] F.Iachello, Phys. Rev. Lett., v.85(2000)3580.

[20] F.Iachello, Phys. Rev. Lett., v.87(2001)052502-1.

[21] N.Pietralla, T.Mizusaki, P.von Brentano, Phys. Rev. C57, 150(1998).

[22] J.Adam, J.Dobeš, M.Honusek, V.G.Kalinnikov, J.Mrázek, V.S.Pronskikh, P.Čaloun, N.Z.Lebedev, V.I.Stegailov, V.M.Tsoupko-Sitnikov, Preprint JINR E6-2001-93, Dubna.

[23] J.Adam, J.Dobeš, M.Honusek, V.G.Kalinnikov, J.Mrázek, V.S.Pronskikh, P.Čaloun, N.Z.Lebedev, V.I.Stegailov, V.M.Tsoupko-Sitnikov, Preprint JINR E6-2001-154, Dubna.

[24] H.Tagziria, M.Elahash, W.D.Hamilton, M.Finger, J.John, P.Malinski, V.N.Pavlov, J. Phys. G16(1990)1323.

[25] R.V.Jolos, P.von Brentano, N.Pietralla, I.Schneider, "Shape invariants in the multiple "Q-excitation" scheme", Nucl.Phys. A618 (1997)126.

[26] Yu.V.Palchikov, P.von Brentano, R.V.Jolos, "Universal description of the 0_2^+ state in collective nuclei", Phys.Rev. C57(1998)3026.

[27] P.O.Lipas, J.Kumpalainen, E.Hammaren, T.Honkaranto, M.Finger, T.I.Kracíková, I.Procházka, J.Ferrencei, Physica Scripta, 27(1983)8-22.

[28] A.Gómez, O.Castanõs, A.Frank, Nucl. Phys. A589(1995)267.

[29] J.Kern, P.E.Garrett, J.Jolie, H.Lehman, Nucl. Phys. A593(1995)21.

[30] P.D.Duval, B.R.Barrett Nucl.Phys.**A376** (1982) 213.

[31] Agda Artna-Cohen Revised A–Chains, A=152 Nucl.Data Sheets **79** (1996) 1.

[32] O.Scholten, DPhil.thesis (University of Groëningen) (1980).

[33] R.F.Casten and N.V.Zamfir, Phys. Rev. Lett. v.85, 3584 (2000).

[34] R.F.Casten and N.V.Zamfir, Phys. Rev. Lett. v.87, 052503 (2001).

Received on January 29, 2002.

Адам И. и др. E6-2002-11
Свойства коллективных состояний ^{152}Gd
(Сравнение эксперимента и теории)

Полученные в эксперименте энергии уровней и приведенные вероятности переходов, разряжающих возбужденные состояния ^{152}Gd, сравниваются с расчетами, выполненными с использованием феноменологических формул, а также моделей Q-фононов, IBA-2, фазовых переходов U(5)–SO(6) и U(5)–SU(3). Приводится сравнение с расчетами, выполненными другими авторами.

Работа выполнена в Лаборатории ядерных проблем им. В. П. Джелепова ОИЯИ.

Препринт Объединенного института ядерных исследований. Дубна, 2002

Adam J. et al. E6-2002-11
Properties of ^{152}Gd Collective States
(Comparison of Experimental and Theoretical Results)

The experimental level energies and reduced probabilities of the transitions decoupling the ^{152}Gd excited states are compared with the calculations using a number of phenomenological formulae, as well as the Q-phonon model, IBA-2, phase transitions U(5)–SO(6) and U(5)–SU(3). A comparison with the calculations made by other authors is also given.

The investigation has been performed at the Dzhelepov Laboratory of Nuclear Problems, JINR.

Preprint of the Joint Institute for Nuclear Research. Dubna, 2002

Макет *Т. Е. Попеко*

ЛР № 020579 от 23.06.97.
Подписано в печать 22.02.2002.
Формат 60 × 90/16. Бумага офсетная. Печать офсетная.
Усл. печ. л. 1,7. Уч.-изд. л. 2,03. Тираж 320 экз. Заказ № 53146.

Издательский отдел Объединенного института ядерных исследований
141980, г. Дубна, Московская обл., ул. Жолио-Кюри, 6.